[American Journal of Science, Vol. 310, December, 2010, P. 1595–1622, DOI 10.2475/10.2010.13]

EARLY ARCHEAN CRUST OF THE MIDDLE DNEPR AND AZOV DOMAINS, UKRAINIAN SHIELD—EVIDENCE FROM AGES OF DETRITAL ZIRCONS IN MESOARCHEAN GREENSTONE BELTS

E. BIBIKOVA*, S. CLAESSON**, A. FEDOTOVA*, G. ARTEMENKO***, and L. ILYINSKY**

ABSTRACT. To clarify the early evolution of the Ukrainian Shield we have dated detrital zircons, separated from metasedimentary rocks of Mesoarchean greenstone belts from the Middle Dnepr and Azov domains (Ukrainian Shield). For the Middle Dnepr domain, the main population of analyzed zircons from three samples of metasediments from the upper Belozerka series of the Verkhovtsevo and Belozerka greenstone belts is in the age range 3.0 to 3.1 Ga, with some crystals as old as 3.2 to 3.3 Ga. The results indicate that the sediment sources were dominated by volcano-plutonic rocks of the belts themselves, with some contribution from basement rocks of the Auli series. For the Azov domain, zircons from four samples of mica schists from the Soroki greenstone belt were analyzed, focusing mainly on cores identified by CL and inner parts of crystals. The data show a group of ages in the range 3.5 to 3.6 Ga. Several zircon cores are older than 3.7 Ga. Overgrowths clearly identified by CL are about 3.2 to 3.0 Ga old. Trace element compositions of the studied metasedimentary rocks (fractionated REE patterns, low HREE contents and negative Nb anomalies) reflect contributions from TTG magmatic series and related volcanic rocks to the sediments, and input from ultramafic-mafic sources is identified using Cr/V and Ni/Co ratios. Sm-Nd model ages of 3.1 to 3.3 and 3.3 to 3.4 Ga for the Middle Dnepr and Azov domains, respectively, and $\varepsilon_{Nd}(T)$ for the analyzed samples, are in a good agreement with the zircon data. Our new results indicate that Paleoarchean crust in the Azov domain was more widely distributed than previously recognized.

Key words: Ukrainian Shield, metasediments, greenstone belt, detrital zircons, cathodoluminescence, isotopic age, Sm-Nd model age, Paleoarchean crust.

INTRODUCTION

To address the question of how and when the earliest Earth crust was formed and evolved, and how widely it was distributed, all new evidence for the existence of such crust is important.

One of the most powerful tools to obtain such information is investigation of accessory zircon. Being resistant to mechanical and chemical influence, zircon is preserved in most magmatic, metamorphic and sedimentary rocks. Zircon contains not only information about its age (U-Th-Pb isotopic systems), but also important geochemical information: the isotope composition of Hf, which substitutes isomorphically for zirconium in the zircon structure, reflects the nature of the source material for the rock in which the zircon crystallized, while the oxygen isotope composition and distribution of rare earth elements (REE) indicate the genesis of minerals in the rock (Peck and others, 2001; Valley and others, 2006). The importance of zircon in the study of the early history of the Earth has increased along with the refinement of isotope geological methods and microanalytical techniques, in particular, the construction of high resolution secondary ion mass-spectrometers, permitting geochronological and geochemical study of zircon in spots less than 20 μm in size.

* Vernadsky Institute of Geochemistry and Analytical Chemistry, Russian Academy of Sciences, Kosygin str. 19, Moscow 119991, Russia; bibikova@geokhi.ru

** Swedish Museum of Natural History, Box 50 007, SE-104 05 Stockholm, Sweden; stefan.claesson@nrm.se

*** Institute of Geochemistry, Mineralogy and Ore Formation of the National Academy of Sciences, Ukraine, Palladin Ave., 34, 03680 Kiev-142, Ukraine

Detrital zircons from old metasedimentary rocks can provide valuable contributions to our knowledge of Earth's early crust. The isotopic and geochemical information enclosed in such crystals can tell us about the primary nature of rocks which may have already disappeared from the Earth's surface, and thus cannot be studied directly. Detrital zircon keeps the isotopic and geochemical information on the primary source of the mineral. The most prominent example is zircons from quartzites and conglomerates of the Mesoarchean (about 3.0 Ga old) greenstone belts in the Yilgarn Craton of Western Australia, which have been used to decipher the age and the primary nature of the earliest (older than 4.0 Ga) Hadean crust of the Earth even though the protolith of these primary rocks has not been preserved (Wilde and others, 2001).

In modern descriptions, the Ukrainian Shield is commonly divided into several blocks or domains, separated by deep-seated fault or suture zones (fig. 1). Archean rocks dominate the granite-greenstone Middle Dnepr domain in the central part of the shield, and high grade metamorphic Archean rocks are also known in the Podolian domain in the west, and in the Azov domain in the east. For many decades it was believed that the protoliths of all these three domains were of Paleoarchean age

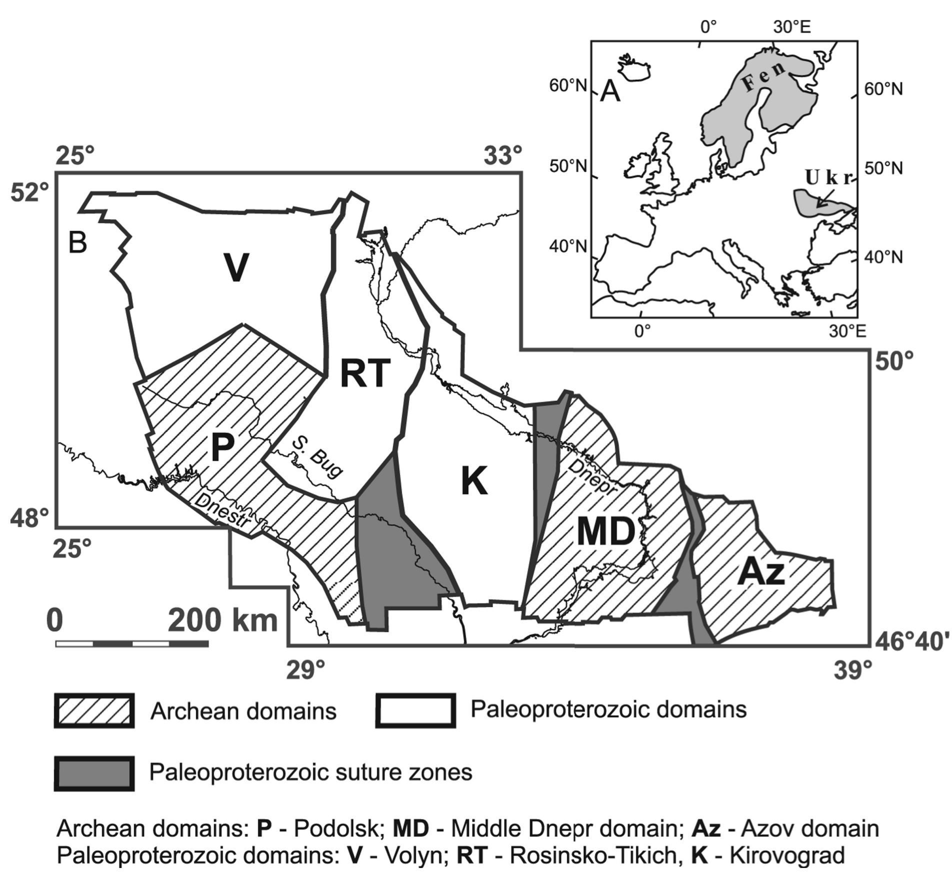

Fig. 1. (A) Location of the Archean-Proterozoic Fennoscandian (Fen) and Ukranian (Ukr) shields of Europe (B). Geological scheme of the Ukrainian Shield after Claesson and others, 2006.

(Scherbak and Bartnitsky, 1995). Detailed geochronological studies of the Middle Dnepr region (Bibikova, 1989; Samsonov and others, 1993, 1996) have not identified any formations older than 3.3 Ga from either rocks of greenstone belts or the basement. Zircons as old as 3.6 to 3.7 Ga have been dated by us from two localities: from tonalities and pyroxenites of the Novopavlovsk complex, recovered from drill holes inside the Orekhovo-Pavlograd tectonic (suture) zone which separates the Azov and the Middle Dnepr domains (Bibikova and Baadsgaard, 1986; Bibikova, 1989; Bibikova and Williams, 1990), and from the western part of the shield, in tonalites and enderbites of the Dnestr-Bug series near the Golovan' suture zone, stretching along the eastern border of the Podolian domain (Claesson and others, 2006) (fig. 1).

As shown by Nutman (2001), metasediments from Meso- and Neoarchean greenstone belts are generally rich sources for identification of ancient zircon. In this study we have made an attempt to further clarify the early crust of the Ukrainian Shield by dating detrital zircons from metasedimentary rocks of Mesoarchean greenstone belts: the Verkhovtsevo and Belozersk belts in the Middle Dnepr domain and the Soroki greenstone belt in the Azov domain (fig. 2).

The primary purpose of this study was to identify and date the oldest components in the zircon populations, and thus clarify the existence of Paleo- or Eoarchean source rocks in the provenance areas of sediments in the two domains. We have focused on the oldest zircon grains and zircon cores, and not attempted to quantify the distribution of variously-aged Archean rocks in the investigated samples.

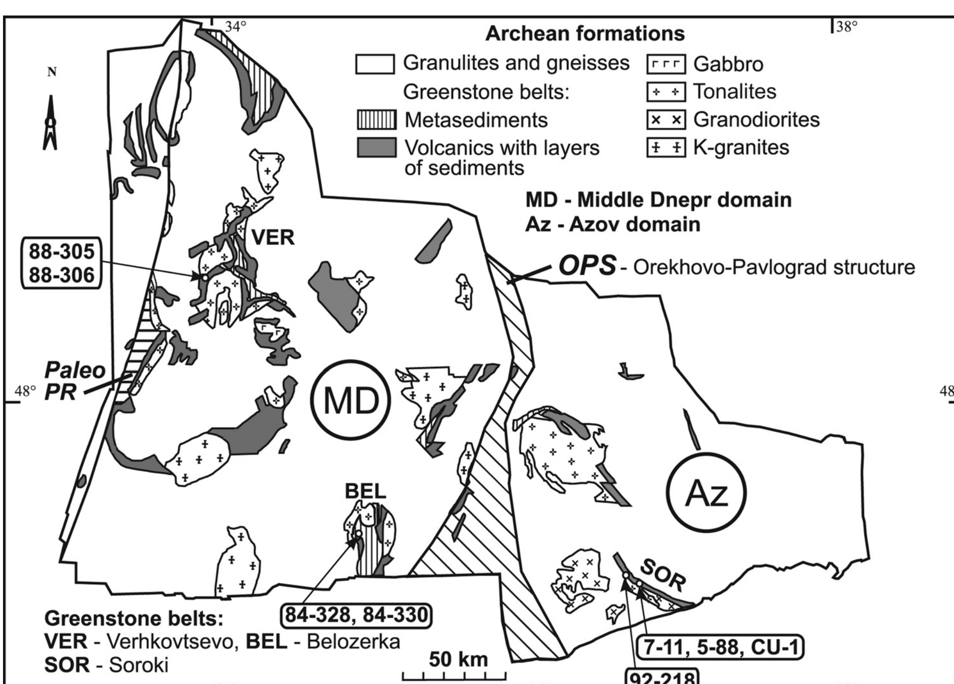

Fig. 2. Geological subdivision of the Dnepr and Azov domains of the Ukrainian Shield with location of metasedimentary rocks sampled in this study. *Paleo PR*-Paleoproterozoic

GEOLOGY

The Middle Dnepr domain.—The domain is a typical granite-greenstone province, with mildly metamorphosed greenstone belt rocks surrounded by higher metamorphic granite-gneiss basement rocks of the Auli series (Shcherbak and others, 1984; Scherback and Ponomarenko, 2000). Several greenstone belts have been recognized inside the Middle Dnepr domain; among them the Belozerka, Konka, Sura, Verkhovtsevo and others (fig. 2). All greenstone belts have similar structure and composition. They are represented by volcano-sedimentary rocks of the lower Konka series and the upper Belozerka series. The lower Konka series (thickness about 15 km), lying directly on the basement rocks, is composed of metamorphosed tholeiitic basalts, komatiites, and banded iron formations. In the upper part of this series, meta-andesites and even more acidic volcanic rocks also occur. The Konka series is unconformably overlain by the Belozerka series represented by meta-terrigenous rocks, mainly shales. Sandstones, meter-thick conglomerate layers and rare banded-iron formations also occur. Volcanic rocks are subordinate.

Syntectonic and post-tectonic granitoids are spatially related with the supracrustal rocks of the greenstone belts. These include TTG (tonalite-trondhjemite-granodiorite) series rocks as old as 3170 to 3100 Ma and younger 2950±50 Ma granites of the Sura complex. Potassium granites were formed about 2800 m.y. ago (Claesson and others, 2006).

The Azov domain.—Greenstone belts in the Azov domain are represented by typically mono- or synclinal, up to 1.5 km wide structures, located in major regional fault zones which have been interpreted to be rifts (Bobrov and others, 2000). Among these are the Soroki and other belts (fig. 2). The Soroki greenstone belt is situated in the SW part of Azov domain (fig. 2) and it is about 35 km long and up to 1.2 km wide. The volcano-sedimentary rocks form a symmetrical syncline with a metamorphic zonation from greenschist to epidote-amphibolite facies.

The volcano-sedimentary rocks of the Soroki belt belong to the Osipenko series. Two suites are recognized: the lower Olgino and the upper Krutobalka suite. The total thickness of the Osipenko series is about 500 m. Volcanic rocks prevail in the Olgino suite and meta-terrigeneous rocks in the Krutobalka suite. The latter is composed of sandstones, conglomerates, and high-Al schists with metamorphic biotite, muscovite, staurolite, sillimanite, tourmaline, and garnet. Rare bodies of amphibolite are also present. A type section across the Soroki belt is located on the right shore of the Berda River, between the ravines Dolzhik in the north and Sobachi in the south (Kon'kov and others, 1980; Scherbak and others, 1995, 2005; Bobrov and others, 2000; Artemenko and others, 2001; Scherbakov, 2005).

The Osipenko series was previously regarded as Proterozoic, but its Archean age was recognized when it was demonstrated that the mafic rocks of the Olgino suite are intruded by 2.8 Ga old granitoids belonging to the Shevchenko complex (Artemenko, 1997). Zircon from garnet-biotite-plagiogneisses underlying the mafic rocks of the Olgino suite has given an age of 3350 Ma (Artemenko, 1997). The Archean age of the Osipenko series is further confirmed by the 2.83 Ga age obtained for granodiorites of the Osipenko massif, which intruded into rocks of the Krutobalka suite (Artemenko and others, 1986).

ANALYTICAL PROCEDURE

U-Pb analysis.—Zircons were separated from 10 to 15 kg samples of metasedimentary rocks from greenstone belts in the Middle Dnepr and Azov domains of the Ukrainian Shield. From the coarse grained zircon fractions (+100 μm) mainly zircons with cores were handpicked and mounted together with the reference zircon 91500 in transparent epoxy resin, polished to expose the interior parts of the crystals and coated with a thin layer of gold. The morphology and inner structure of zircons was studied in reflected and transmitted light, and by SEM cathodoluminescence (CL) imaging.

U-Th-Pb dating was performed using the Cameca 1270 secondary ion mass-spectrometer at the Nordsim laboratory, Swedish Museum of Natural History in Stockholm, Sweden. The analytical method and data regression technique have been described in detail by Whitehouse and others (1997, 1999), and Whitehouse and Kamber (2005). Material was sputtered from selected areas of the polished sample surface using an O^{-2} primary beam, which was adjusted to produce even sputtering over an ellipsoid area of ca. 20×25 μm. The analysis of secondary ions was done with a mass resolution of ca. 5600 in order to separate Pb^{+} ions from molecular interferences. During analysis, the source chamber was flooded with O_2 gas in order to enhance the Pb^{+} yield. The accuracy for the lead isotopic composition was 0.1 to 0.3 percent, for U-Pb isotopic ratios 1 to 3 percent.

Since the primary objective of this study was to identify and date the oldest grains in the zircon populations, the isotopic analyses were done in two steps. In the first step only lead isotopic compositions were determined in selected spots and $^{207}Pb/^{206}Pb$ ages were calculated. This age gives an estimate of the real age of the mineral, which is more or less accurate depending upon post-crystallization disturbance of the U-Pb isotopic system in the investigated zircon. When such disturbances in the U-Pb isotopic system occurred recently the $^{207}Pb/^{206}Pb$ age still gives a good estimate of the true age of the mineral, while it may be much younger than the true age if the disturbance was old. Based on the preliminary $^{207}Pb/^{206}Pb$ data, full U-Th-Pb analysis was selected for grains with the highest $^{207}Pb/^{206}Pb$ ages. This procedure permitted an efficient use of available analytical time. The duration for a Pb isotope analysis was 3 minutes, 5 times shorter than for a full U-Pb isotopic analysis, but the precision was, of course, worse.

Sm-Nd analysis.—Nd isotope analyses were obtained using conventional methods at the isotope laboratory at the Vernadsky Institute of Geochemistry and Analytical Chemistry RAS, Moscow. 20 to 30 mg of sample mixed with $^{150}Nd+^{149}Sm$ tracer was dissolved in $HF+HNO_3$ (5:1) in sealed teflon beakers at 200 °C. After decomposition the solution was evaporated and the precipitate was transformed to chloride form. The separation of Sm and Nd was carried out in two steps by ion exchange chromatography. In the first stage the REE enriched fractions were obtained on columns containing cationic exchange resin DOWEX 50W-X8; at the second stage Sm and Nd were separated using HDEHP reagent. The isotope composition of Nd was measured using a multicollector Triton mass spectrometer. The La Jolla Nd standard yielded a $^{143}Nd/^{144}Nd$ ratio of 0.511857±7 (2σ, n=21). The blank was 0.03 ng for Sm and 0.1 ng for Nd. The precision was 0.1 percent for $^{147}Sm/^{144}Nd$ and better than 0.005 percent for $^{143}Nd/^{144}Nd$. The measured $^{143}Nd/^{144}Nd$ ratio was normalized to $^{148}Nd/^{144}Nd\equiv0.241572$, corresponding to $^{146}Nd/^{144}Nd=0.7219$. The model ages (T_{DM}) were calculated using the following values for the depleted mantle: $^{143}Nd/^{144}Nd=0.513151$, $^{147}Sm/^{144}Nd=0.2136$ (Goldstein and Jacobsen, 1988).

RESULTS

Middle Dnepr domain.—We have studied three samples of zircons separated from metasediments from the Belozersk series in the Belozersk and Verkhovtsevo greenstone belts of the Middle Dnepr domain (fig. 2). According to Stratigraphic crossections in the Precambrian of the Ukrainian Shield (Scherbak, editor, 1985) these two series are present in all greenstone belts of the Middle Dnepr domain.

In the Verkhovtsevo greenstone belt metasandstone samples 88-305 and 88-306 were taken from drill-hole 0708, situated at 48°23′56″N and 33°59′56″E. Sample 88-305 was taken from the interval 165.5 to 175.5 m and sample 88-306 from 190 to 205 m. Both samples consist of quartz grains (about 50%) in a cement composed of fine grained quartz (95%), muscovite (5%) and single grains of garnet, amphibole and zircon.

In the Belozerka greenstone belt quartz metasandstones 84-328 and 84-330 were sampled from the "Dneproruda" mine, situated at 47°10′58″N and 34°57′58″E, at a depth of 640 m. Samples were taken from the same metasandstone layer about 5 m from each other. Samples represent mature sediment and consist of well–rounded quartz grains (40%). The cement (60%) is composed of muscovite (25%), fine-grained quartz (70%) and carbonate (5%).

The major and trace element compositions of these rocks are presented in table 1. Figures 3A and 3C are chondrite-normalized REE and primitive mantle diagrams, respectively, for the studied sediments compared with those for different rock types. The PAAS (Post-Archean Australian average shale, Nance and Taylor, 1976) chondrite-normalized pattern ($La_N/Yb_N=9.2$) is typical for continental derived sediments as shown by Taylor and McLennan (1985), and the REE pattern for the average Archean Jack Hills metasediments (Maas and McCulloch, 1991) shows a slightly steeper slope ($La_N/Yb_N=16$). The studied metasediments have fractionated (La_N/Yb_N from 12 to 30) REE patterns with low HREE contents (Yb lower than 2 ppm and Y lower than 6 ppm). We explain these features as indicating a source of TTG composition, with typical strongly fractionated REE patterns and low concentrations of Y and HREE (Martin and others, 2005).

The trace element compositions (fig. 3C) are compared with the average TTG older than 3.0 Ga (Martin and others, 2005) and with dacite from the Verkhovtsevo greenstone belt, which occurs in association with tonalite, trondjemites and rhyolite (Samsonov and others, 1993). The studied metasediments, TTG and the dacite, all have fractionated trace element compositions and negative Nb anomalies. These data suggest that contributions from TTG magmatic series and related volcanic rocks to the sedimentation are clearly identified. The Cr/V and Ni/Co values in the studied rocks (higher than 3.4 and 3.6 respectively, table 1) are higher than those both in the PAAS (0.7 and 2.4) and in the Archean shale (1.5 and 2.5), which may indicate the presence of komatiites in the denudation region (Taylor and McLennan, 1985).

Zircons in the metasandstone are typically prismatic, commonly with oscillatory zoning, and are slightly rounded. These features correspond to zircons from magmatic rocks of acid-intermediate composition. CL images of zircons are generally rather dark (fig. 4).

As mentioned above, the isotopic analyses were done in two steps. In the first step $^{207}Pb/^{206}Pb$ analysis was done on more than 60 zircon crystals. The results of the first step analyses are given in table A1 in the Appendix, and are included in the age histogram in figure 5B. The results from the second step of analysis, which provide a basis for more reliable estimates of the ages of the detrital zircons, are given in table 2 and shown in figures 5A and 5B.

As shown in table 2, the uranium concentrations in zircons are generally rather low, commonly lower than 100 ppm. For crystals with U concentration higher than 200 ppm, the discordancy of age values sharply increases with few exceptions, reaching more than 80 percent when uranium concentration is as high as 1000 ppm. But this discordancy only affects very slightly the age values calculated from the $^{207}Pb/^{206}Pb$

TABLE 1

Chemical composition of metasedimentary rocks from greenstone belts in the Middle Dnepr (1-3) and Azov (4-7) domains of the Ukrainian Shield

Oxide, %	(1) 84-328	(2) 88-305	(3) 84-330	(4) 7-11	(5) 7-12	(6) 5-88	(7) 92-218
SiO_2	70.93	90.08	86.73	71.72	71.54	74.98	72.40
TiO_2	0.35	0.15	0.33	0.43	0.46	0.57	0.74
Al_2O_3	13.42	5.65	5.56	13.42	13.31	11.16	12.10
Fe_2O_3	0.65	0.89	1.28	0.83	0.19	1.41	1.40
FeO	3.02	0.64	1.23	3.72	4.07	2.51	2.60
MnO	0.07	traces	0.03	0.03	0.01	0.10	0.06
MgO	1.57	traces	0.73	1.52	1.42	1.14	2.30
CaO	1.41	0.70	0.38	2.01	2.12	1.77	1.50
Na_2O	0.55	0.14	0.25	3.82	4.26	2.60	2.40
K_2O	2.50	1.00	0.90	1.22	1.25	1.42	1.80
P_2O_5	0.01	0.005	0.11	0.09	0.10	0.19	0.05
H_2O-	-	0.08	0.06	0.11	0.09	0.18	0.70
LOI	1.72	1.01	1.71	0.72	0.72	2.21	1.68
Total	99.76	100.34	99.98	99.66	99.56	100.24	99.87
ppm							
Ba	477	205	175	601	645	580	577
Sr	56.5	18.2	23.9	259	174	151	124
Co	14.9	6.3	4.9	10.9	9.1	9.7	16.5
Cr	158	96.5	62.9	103	90.2	78.1	144
Cs	3.5	0.3	1.0	2.5	2.0	0.9	2.6
Hf	5.3	1.9	2.5	2.3	2.7	3.4	2.5
Nb	6.5	1.2	1.6	4.2	4.8	3.7	4.4
Ni	53.1	59.3	25.4	38.3	31.4	21.2	62.8
Rb	65.2	21.2	23.6	39.1	7.4	21.4	61.0
Sc	7.2	1.3	2.0	6.8	5.8	5.7	9.4
Th	14.1	2.8	7.0	5.8	5.6	6.6	5.0
Ti	1986	460	583	1932	2011	1575	2223
V	46.6	9.7	12.6	49.5	48.2	42.6	64.0
Y	6.9	2.1	4.8	5.0	4.6	5.4	3.9
Zn	13.7	traces	1.9	26.5	27.8	23.3	42.9
Zr	200	76.3	94.3	85.6	103	104	87.7
La	48.29	21.96	15.17	26.94	33.51	29.63	21.50
Ce	107.02	62.54	41.92	83.89	62.40	79.63	58.41
Pr	11.43	6.59	4.83	9.23	6.81	8.55	6.44
Nd	37.86	21.65	17.67	33.67	24.08	29.69	23.03
Sm	5.72	2.84	3.14	5.38	3.87	4.96	3.87
Eu	1.54	0.80	0.84	2.01	1.33	1.53	1.57
Gd	5.13	2.40	2.72	4.83	3.47	4.65	3.32
Tb	0.60	0.25	0.34	0.62	0.43	0.58	0.44
Dy	2.67	0.90	1.52	2.78	1.84	2.65	1.79
Ho	0.55	0.16	0.27	0.51	0.31	0.51	0.30
Er	1.78	0.56	0.78	1.39	0.91	1.46	0.86
Tm	0.26	0.07	0.12	0.16	0.12	0.21	0.11
Yb	1.73	0.49	0.81	1.08	0.70	1.32	0.68
Lu	0.27	0.08	0.13	0.15	0.11	0.19	0.10
La_N/Yb_N	18.9	30.3	12.7	16.9	32.3	15.2	21.4
Cr/V	3.4	9.9	5.0	2.1	1.9	1.8	2.3
Ni/Co	3.6	9.4	5.2	3.5	3.5	2.2	3.8

1—mica schist (84-328), Belozerka greenstone belt, mine, level 640 m, Belozerka series; 2—metasandstone (88-305), Verkhovtsevo greenstone belt, hole 0708, depth 165.5–175.5 m, Belozerka series; 3—metasandstone (84-330), Belozerka greenstone belt, mine, level 640 m, Belozerka series; 4—mica schist (7-11), Soroki greenstone belt, Krutobalka suite, Sobachya gully; 5—the same (7-12); 6—the same (5-88); 7—paragneiss (92-218), Soroki greenstone belt, Krutobalka suite, Village Soroki, right shore of Burtichnya River.

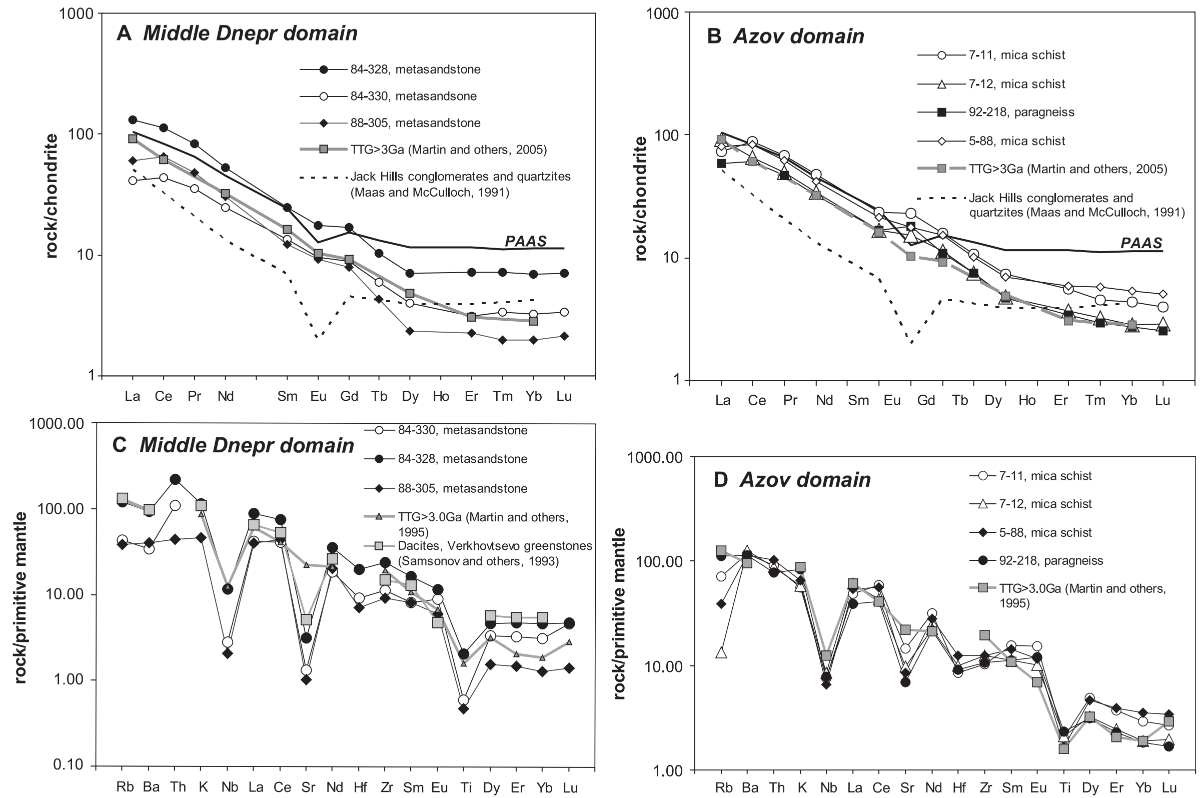

Fig. 3. Chondrite normalized REE patterns and primitive mantle normalized multi-element diagrams for the clastic metasediments from Middle Dnepr (A and C) and Azov (B and D) domains compared with the average TTG older than 3.0 Ga (Martin and others, 2005). The average REE composition of Archean detrital metasedimentary rocks from Jack Hills belt, Western Australia (Maas and McCulloch, 1991) and PAAS (post-Archean Australian average shale, see Nance and Taylor, 1976) are also plotted in figs. 3A and 3B. The trace element composition of dacite from the volcanic sequence of the Verkhovtsevo greenstone belt related to the TTG suite of the Middle Dnepr domain (Samsonov and others, 1993) is plotted in fig. 3C. The shape of the PAAS chondrite normalized REE pattern is typical for continental derived sediments, as shown by Taylor and McLennan (1985), and the REE pattern for the Archean Jack Hills metasediments shows a similar shape. The studied metasediments have highly fractionated REE patterns, explained by the influence of a source with a TTG composition. Normalizing values are from Taylor and McLennan (1985).

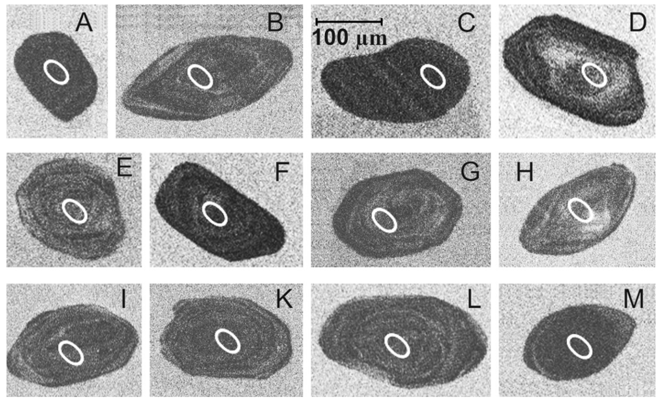

Fig. 4. Cathodoluminescence images of some zircons from metasediments of the Middle Dnepr domain: A—sample 305, grain 7; B—sample 328, grain 22; C—sample 330, grain 16; D—sample 330, grain 21; E—sample 330, grain 3; F—sample 330, grain 9; G—sample 328, grain 14; H—sample 328, grain 19, I—sample 328, grain 28; K—sample 305, grain 4; L—sample 305, grain 11; M—sample 305, grain 15. Ellipses mark site of SIMS analyses and data are presented in table 2.

isotopic ratios (table 2, fig. 5A), indicating that the discordancy was mainly caused by recent lead-loss. Bibikova (1989) has shown this to be a typical feature for zircons from the Middle Dnepr domain. The low uranium concentrations in most zircons demonstrate that their dark CL appearances are not correlated with the uranium concentrations but caused by some other feature, possibly the high concentrations of REE.

In spite of the high discordance of isotopic ages in many spots, most $^{207}Pb/^{206}Pb$ ages form a distinct group in the time span 3.00 to 3.15 Ga (table 2), which corresponds to the ages of zircons from volcano-plutonic rocks of the belts themselves (Samsonov and others, 1993). More than 10 zircons have $^{207}Pb/^{206}Pb$ ages of 3.2 to 3.3 Ga (figs. 4B-D), corresponding to the maximum age of zircons from the Auli basement series (Samsonov and others, 1993, 1996). Zircons from the age group 3.2 to 3.3 Ga are the most concordant (table 2, fig. 4A). One zircon core was older than 3.5 Ga (fig. 4A), being nearly concordant (less than 3% discordance). In appearance and inner structure this zircon is similar to all other crystals. It is prismatic, rounded, and nearly black in CL with a slightly lighter core. The concentrations of U and Th are rather low; the Th/U ratio is 0.28.

The Sm-Nd model ages of the whole rock samples (3.1-3.3 Ga) and $\varepsilon_{Nd}(T)$ for the few analyzed samples (table 3) are in a good agreement with the zircon data. For the $\varepsilon_{Nd}(T)$ calculation the deposition ages for the sediments was set at 3.0 Ga, in accordance with Samsonov and others (1993) and Scherbak and others (2005).

Azov domain.—We have studied 4 samples of zircons separated from metasedimentary rocks of the Krutobalka suite from the Soroki greenstone belt (fig. 2). Three samples, 5-88, 7-11, and CU-1, were taken from the Sobach'ya gully (46°57′58″N and 36°49′39″E); sample 92-218 was taken near the village of Soroki (47°03′17″N and 36°41′17″E). The samples from the Sobach'ya gully were taken from the same outcrop (5×10 m) during field work in 2002 (5-88 and 7-11) and in 2008 (CU-1). The outcrop is quite homogeneous and consists mainly of mica schists. These are gray, generally schistose rocks with lepido- to granoblastic texture. They consist of 15 to 20 percent biotite, 40 to 45 percent plagioclase (albite-oligoclase), 40 percent quartz, and minor chlorite, apatite and single grains

Table 2

Isotopic data for metasediments for the Middle Dnepr greenstone belts

Spot number	Concentration, ppm			Th/U	f_{206} %(1)	Isotopic ratios				Age, Ma		Discordance
	U	Th	Pb			$^{206}Pb/^{238}U$	±σ	$^{207}Pb/^{235}U$	±σ	$^{207}Pb/^{206}Pb$	±σ	%
88-330, metasandstone, Belozerka greenstone belt, Belozerka series												
330-2	56	28	53	0.511	0.13	0.6845	0.93	23.946	1.06	3208	8	3
330-3	86	97	84	1.192	0.05	0.6268	0.89	20.098	0.99	3070	7	1
330-4	162	124	117	0.606	0.25	0.5084	0.93	15.946	1.00	3034	6	-13
330-5	296	352	127	0.293	3.15	0.3033	0.91	10.460	1.05	3185	8	-50
330-7	65	32	53	0.462	0.15	0.5959	0.88	18.981	1.02	3059	8	
330-8	181	122	139	0.483	0.18	0.5616	0.88	17.924	1.01	3062	8	-5
330-9	124	124	106	0.827	1.87	0.5800	0.88	18.409	1.03	3053	8	-2
330-10	1128	590	234	0.148	1.31	0.1429	0.90	5.278	1.06	3293	4	-77
330-12	62	36	45	0.437	0.41	0.5278	0.88	16.799	0.99	3058	10	-10
330-15	175	178	139	0.847	0.87	0.5343	0.89	16.850	1.10	3043	7	-9
330-16	78	76	74	0.911	0.21	0.6255	0.89	22.452	0.99	3249	8	-2
330-17	59	29	45	0.452	0.23	0.5633	0.89	17.827	1.04	3049	13	-3
330-20	177	134	121	0.510	0.64	0.4846	0.88	15.431	1.19	3058	6	-18
330-21	75	26	61	0.314	0.20	0.6017	0.88	21.435	0.97	3237	8	-5
84-328, metasandstone, Belozerka greenstone belt, Belozerka series												
328-4	351	172	116	0.235	0.12	0.2300	0.89	8.160	0.96	3230	5	-63
328-5	47	20	39	0.371	0.35	0.6127	0.88	21.682	1.07	3226	9	-3
328-6	201	115	126	0.496	0.11	0.4446	0.90	14.000	1.34	3041	5	-24
328-7	132	67	78	0.378	0.14	0.4299	0.89	13.506	0.97	3036	6	-27
328-8	51	39	48	0.728	0.15	0.6401	1.31	23.011	1.08	3251	10	-1
328-9	164	85	108	0.455	0.28	0.4740	0.88	14.879	1.04	3036	6	-20
328-14	57	29	45	0.471	0.14	0.5756	0.88	18.278	1.04	3054	8	-2
328-16	112	65	90	0.557	0.15	0.5830	0.98	18.629	0.95	3064	6	-2
328-18	43	32	30	0.403	0.42	0.4974	0.89	17.498	1.16	3217	10	-20
328-19	61	24	46	0.369	0.16	0.5669	0.88	18.045	1.03	3058	9	-4
328-21	383	293	174	0.517	0.14	0.3015	0.95	9.518	1.00	3045	5	-49
328-22	94	49	78	0.488	0.12	0.5949	0.88	20.758	0.98	3204	7	-5
328-24	147	53	52	0.231	0.46	0.2606	0.94	8.191	1.05	3038	9	-54

TABLE 2
(continued)

Spot number	Concentration, ppm U	Th	Pb	Th/U	f_{206} %(1)	$^{206}Pb/^{238}U$	Isotopic ratios ±σ	$^{207}Pb/^{235}U$	±σ	Age, Ma $^{207}Pb/^{206}Pb$	±σ	Discordance %
84-328, metasandstone, Belozerka greenstone belt, Belozerka series												
328-25	169	79	129	0.439	0.08	0.5609	0.89	17.813	0.95	3054	5	-5
328-28	128	57	96	0.426	0.16	0.5560	0.95	17.670	1.02	3056	6	-6
328-30	148	80	73	0.399	0.17	0.3465	1.00	10.940	1.10	3045	7	-41
88-305, metasandstone, Verkho vtsevo greenstone belt, Belozerka series												
305-1	94	103	64	0.955	0.44	0.4352	0.99	13.655	1.09	3035	7	-25
305-3	236	57	76	0.139	1.48	0.2387	0.96	8.028	1.04	3145	6	-60
305-4	72	38	64	0.571	0.08	0.6390	0.88	20.376	0.97	3061	6	3
305-4a(2)	92	54	85	0.596	0.14	0.6579	0.89	23.260	0.96	3225	6	
305-7	195	53	186	0.280	0.06	0.6886	0.89	29.142	0.92	3506	3	-3
305-9	237	99	184	0.432	0.02	0.5808	1.01	17.743	1.03	2992	4	
305-11	170	111	156	0.656	0.08	0.6381	0.98	22.872	1.03	3246	5	-1
305-12	89	35	67	0.372	0.23	0.5640	0.89	17.777	0.96	3042	6	-4
305-13	193	72	107	0.259	0.11	0.4179	2.65	13.242	2.67	3051	5	-27
305-14	203	69	156	0.304	0.05	0.5705	0.88	19.981	0.92	3210	4	-10
305-15	587	20	459	0.037	0.07	0.6189	0.94	21.454	0.95	3194	2	-2

1—f_{206}%, percentage of ^{206}Pb attributed to common Pb, which is calculated from measured ^{204}Pb; 2—a=repeated analysis.

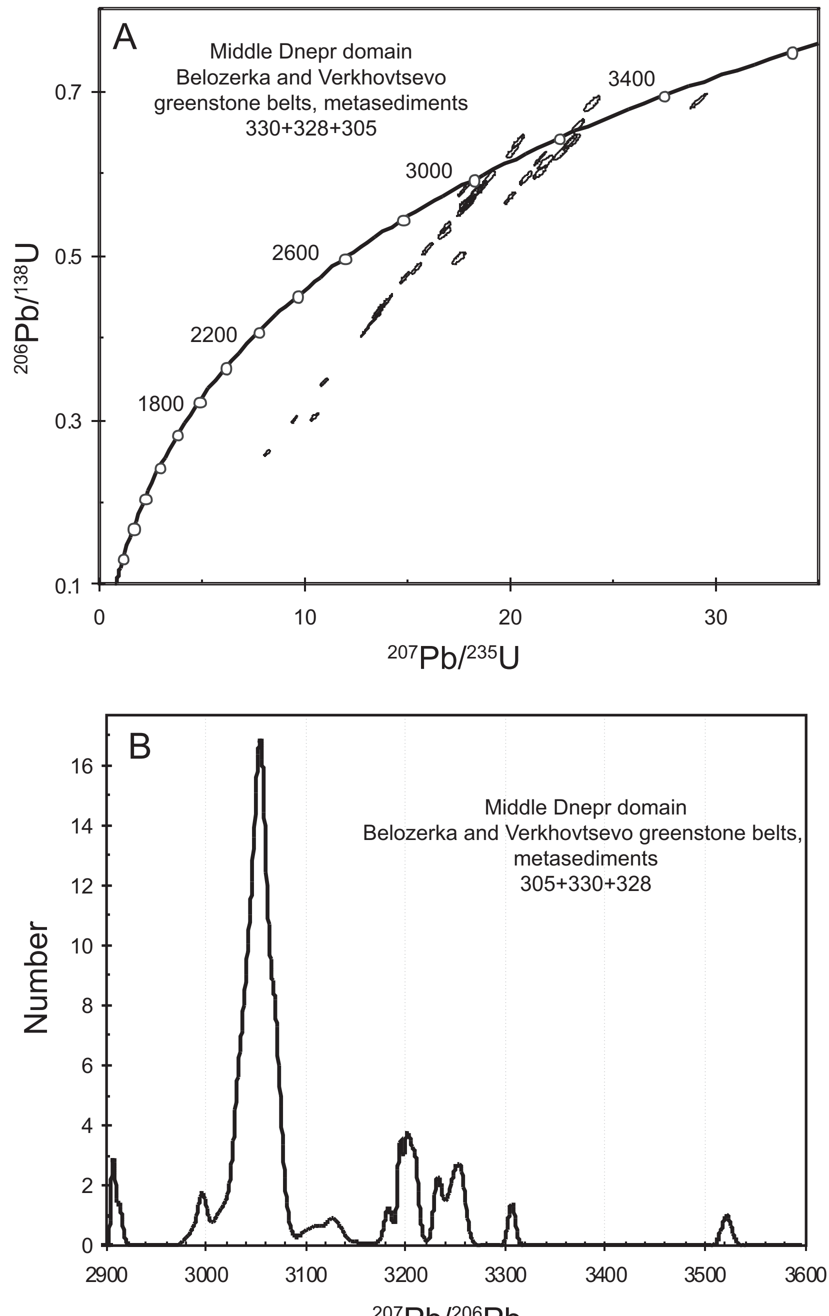

Fig. 5. (A) Concordia diagram for zircons from metasediments of the Belozersk series (samples 305, 328, 330). (B) $^{207}Pb/^{206}Pb$ age histogram for zircons from metasediments of the Belozersk series (samples 305, 328, 330, including all data. From table A1).

of zircon. Sample 92-218 is a paragneiss, consisting of 55 to 60 percent plagioclase (albite), 15 percent biotite, 5 percent muscovite, 20 percent quartz and some carbonate.

Major and trace element compositions of the studied samples are presented in table 1 and illustrated in figures (figs. 3B and 3D). The metasedimentary rocks of the Azov domain represent mature sediments with high SiO_2 contents. The trace element compositions show a similarity with those of the samples from the Middle Dnepr domain: REE patterns are strongly fractionated (La_N/Yb_N from 17 to 32), and a primitive mantle normalized multi-element diagram exhibits negative Nb anomalies. These features are similar to those for TTG series rocks but differ from both PAAS and Jack Hills sediments (figs. 3B and 3D). The Cr/Ni and Co/V ratios (higher than 1.8-2.3 and 2.2-3.8, respectively, table 1) are lower than those in the rocks from the Middle Dnepr domain, but higher than or similar to those in PAAS (0.7 and 2.4) and Archean Shales (1.5 and 2.5) (Taylor and McLennan, 1985). This suggests that mafic-ultramafic rocks were exposed in the source region of these sediments, but contribution from such sources was less important than in the investigated sediments from the Middle Dnepr region.

Zircons separated from the metasediments of the Krutobalka suite are of variable morphological appearance, ranging from well-preserved prismatic grains to ellipsoidal and more irregular. CL imaging reveals variable, commonly complex internal structures with cores commonly displaying oscillatory zoning and one or several overgrowths. Some images of analyzed crystals are shown in figure 6. Most crystals with metamorphic overgrowths are also rounded, indicating that the metamorphic overgrowth occurred before sedimentation.

The isotopic U-Th-Pb dating of zircon from the Soroki greenstone belt was performed in two steps in the same way as the zircon from the Middle Dnepr domain. In the first step, $^{207}Pb/^{206}Pb$ ages were calculated for more than 100 zircon crystals, mainly from cores. These results are given in a table in the Appendix, but are included in the age histogram in figure 7B. Based on these results, crystals with the oldest $^{207}Pb/^{206}Pb$ ages were selected for full U-Th-Pb isotopic analysis. The results are given in table 4 and shown in figures 7A–D. About 40 percent of the zircon cores have $^{207}Pb/^{206}Pb$ ages above 3500 Ma, and the ages of 4 cores exceed 3700 Ma (figs. 7A-D). The uranium concentrations in the oldest cores are 150 to 320 ppm, the Th/U ratios 0.4 to 0.7. Zircons in the 3.5 to 3.6 Ga age group (fig. 7D) have rather low U concentrations (100-200 ppm) and Th/U ratios of about 0.5. The overgrowths are of two types—high and low-U. The ages of zircon overgrowths (as shown in figs. 6F-I) can be estimated at about 3.2 to 3.3 Ga (table 3, fig. 7D), for the least discordant overgrowths, and most have $^{207}Pb/^{206}Pb$ ages of c. 3.3 Ga. The uranium concentrations in light CL zones are less than 100 ppm, with Th/U ratios 0.5 to 0.7. In dark CL grains and overgrowths U concentrations are much higher, with lower Th/U ratios and highly discordant ages.

Four analyzed zircons from sample 92-218, collected near the village of Soroki, form a distinct, only slightly discordant group with $^{207}Pb/^{206}Pb$ ages of 3.05 to 3.08 Ga (fig. 7D). These are low-uranium, rounded zircons with a characteristic CL zonation and without cores (figs. 6L and 6M), and may have crystallized during a metamorphic event which has not been registered in the other Soroki samples, although the Th/U ratios are not low as is typical of metamorphic zircon.

The Sm-Nd model ages and $\varepsilon_{Nd}(T)$ values are shown in table 4. The model ages are in the range 3.3 to 3.4 Ga. 3.1 Ga was chosen as a probable age of sediment deposition (T) for calculating εNd (T). It is not very precise but lies between 3.2

TABLE 3

Sm-Nd isotopic study of metasediments from the greenstone belts in the Middle Dnepr and Azov domains, Ukrainian Shield

Sample Number	Rock	Concentration, ppm		Isotopic ratios			T(DM), Ga	εNd(T)
		[Sm]	[Nd]	$^{147}Sm/^{144}Nd$	$^{143}Nd/^{144}Nd$	± 2σ		
Greenstone Belts of the Middle Dnepr domain, Belozerka series								T(sedimentation) =3.0 Ga
84-328	metasandstone	3.1	22.3	0.0839	0.510504	0.000009	3.1	+2.0
84-330	metasandstone	1.4	10.7	0.0811	0.510428	0.000008	3.2	+1.6
88-306	metasandstone	3.7	20.1	0.1124	0.510999	0.000009	3.3	+0.6
Soroki greenstone belt, Azov domain, Krutobalka suite								T(sedimentation) =3.1 Ga
7-12	mica schist	2.9	18.5	0.0953	0.510626	0.000012	3.3	+1.3
7-11	mica schist	2.1	13.1	0.0972	0.510589	0.000008	3.4	-0.2
5-88	mica schist	2.2	13.7	0.0985	0.510584	0.000005	3.4	-0.8
CU-1	mica schist	2.5	15.7	0.0966	0.510546	0.000003	3.4	-0.8

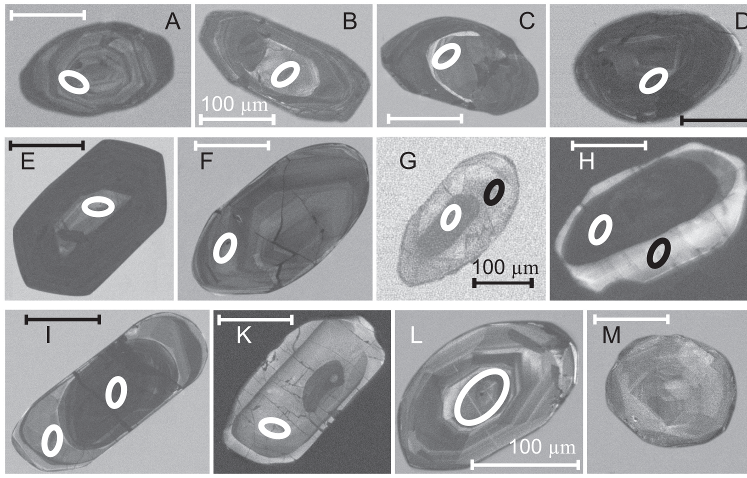

Fig. 6. Cathodoluminescence images of some zircons from metasediments of the Soroki greenstone belt, Azov domain: A—sample CU-1, grain 21; B—sample 5-88, grain 8; C—sample 5-88, grain 14; D—sample CU-1, grain 39; E—sample CU-1, grain 8; F—sample CU-1, grain 5; G—sample CU-1, analysis 38,39 (table 4), H—sample CU-1, analysis 19, 20 (table 4); I—sample CU-1, analysis 10,12 (table 4); K—sample CU-1, grain 35, L—sample 92-218, grain 11; M—sample, 92-218, grain 23. Ellipses mark site of SIMS analyses and data are presented in table 2.

Ga, the age of the youngest detrital zircon grain, and 2.98 Ga, which is the age for crosscutting granites (Artemenko and others, 2001; Bibikova and others, 2008).

DISCUSSION

Our new results demonstrate similarities, but also distinct differences, in the Archean evolution of the Middle Dnepr and Azov domains of the Ukrainian Shield, both with regards to ages of original crustal formation and subsequent development.

The geochemistry of metasediments in both domains indicates that the eroded source regions were composed mainly of TTG series rocks and their volcanic analogues, with some involvement of rocks of mafic-ultramafic composition, as shown by high Cr/V and Ni/Co ratios. The mafic signature is more pronounced in the Middle Dnepr domain. Compared to the PAAS composition and to rocks of Archean greenstone belts in other parts of the globe, such as parts of the Western Australian Yilgarn Craton (Maas and McCulloch, 1991), the Ukrainian Shield rocks investigated in this study are characterized by highly fractionated REE distributions, negative Nb anomalies and the absence of Eu anomalies. Variable quartz concentrations in detrital material influences the concentration levels of trace elements, but not their relative concentrations or characteristic patterns as shown in figure 3.

The trace element patterns of metasedimentary rocks from the Azov and Middle Dnepr domains presented here are similar and consistent with dominant source components of TTG composition. However, the ages of the detrital components are distinctly different.

The Middle Dnepr domain does not appear to have formed earlier than the latest Paleoarchean and Mesoarchean because no zircons older than 3.3 Ga (with

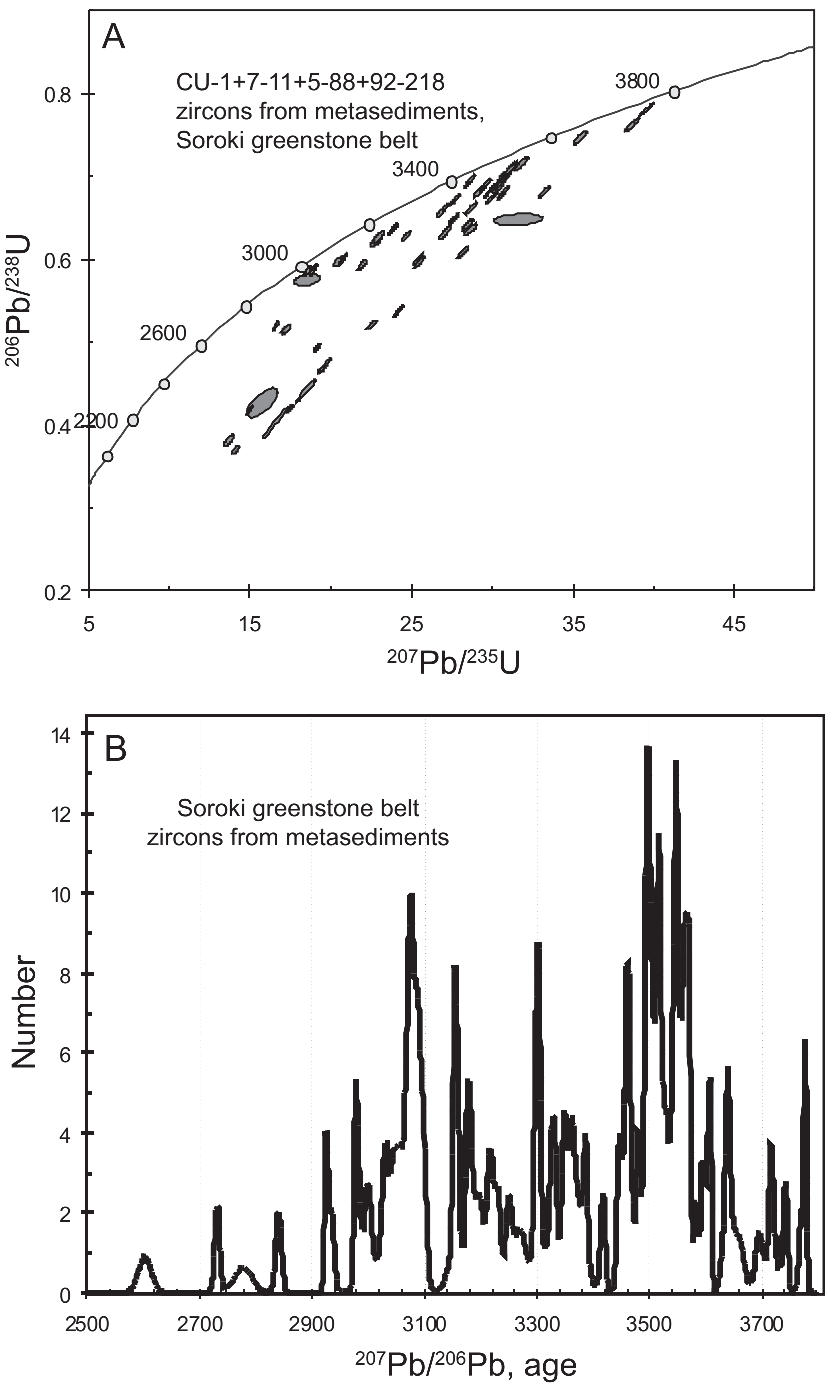

Fig. 7. (A) Concordia diagram for zircons from metasediments of the Krutobalka suite, Soroki greenstone belt, the Azov domain, samples: CU-1, 7-11, 5-88, 92-218. (B) $^{207}Pb/^{206}Pb$ age histogram for zircons from metasediments, samples CU-1, 7-11, 5-88, 92-218 including data from Appendix table A1.

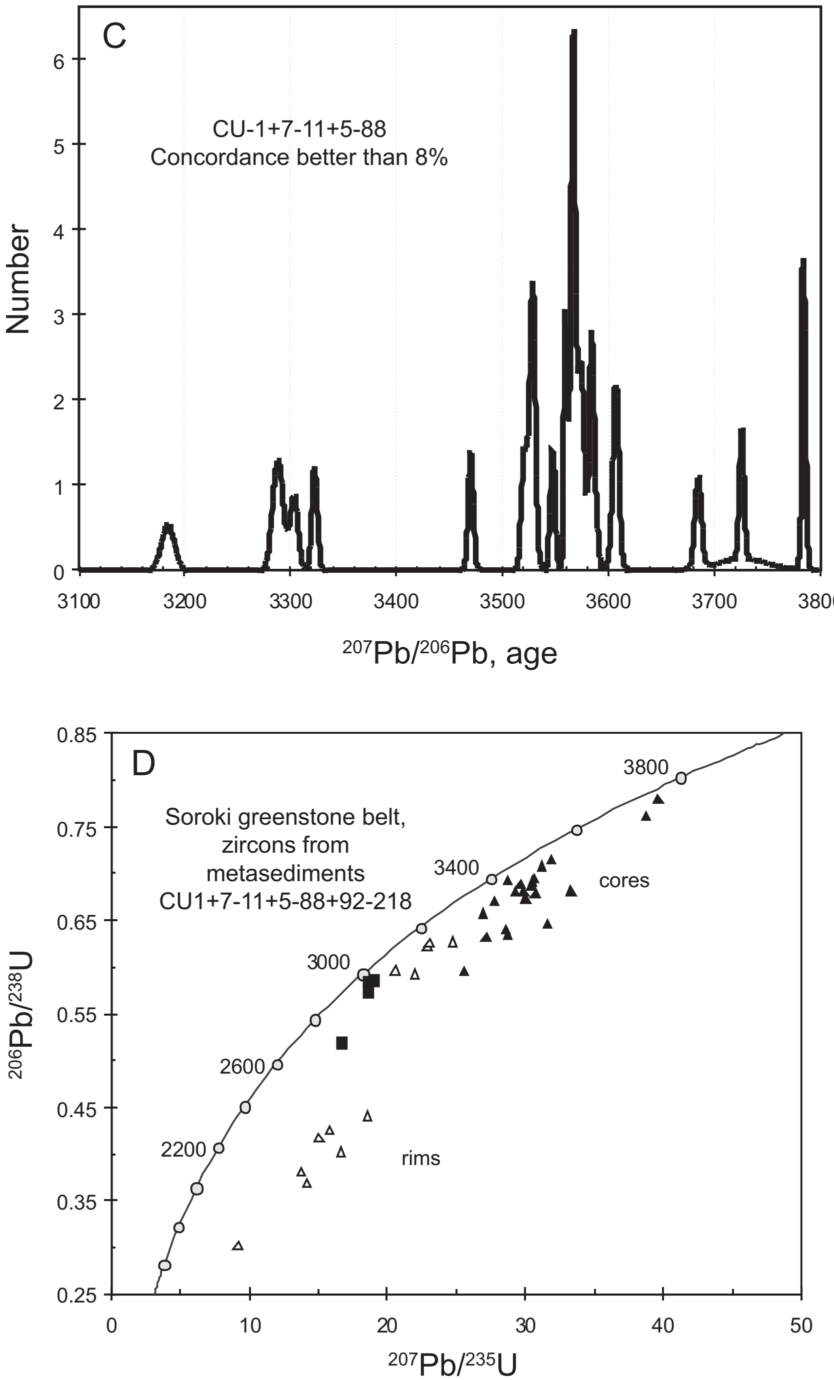

Fig. 7 (continued). (C) $^{207}Pb/^{206}Pb$ age histogram for zircons with the most concordant ages (discordance less than ≤8%) from metasediments CU-1, 7-11, 5-88. (D) Concordia diagram for zircons from samples CU-1, 7-11, 5-88, 92-218: filled triangles—cores; open triangles—rims, filled squares—grains from sample 92-218.

TABLE 4

Isotopic data for zircons from metasediments of The Soroki greenstone belt, Azov domain

Spot number	Concentration, ppm			Th/U	f_{206} %(1)	Isotopic ratios				Age, Ma		Discordance
	U	Th	Pb			$^{206}Pb/^{238}U$	±σ	$^{207}Pb/^{235}U$	±σ	$^{207}Pb/^{206}Pb$	±σ	%
CU-1, mica schist												
CU1-3, c(2)	202	96	193	0.47	0.54	0.6609	0.93	28.740	0.80	3547	4	-8
CU1-5, c	62	34	64	0.55	0.06	0.7099	0.90	31.264	0.79	3567	5	-2
CU1-6, c	213	270	246	1.27	0.05	0.6961	0.94	30.799	0.77	3574	4	-4
CU1-7, c	69	59	63	0.85	1.17	0.6075	0.87	28.217	0.83	3648	6	-18
CU1-8, c	71	47	81	0.66	0.07	0.7458	0.88	35.473	0.82	3684	6	-1
CU1-9 c	62	43	65	0.70	0.04	0.7004	0.88	30.785	0.81	3564	6	-3
CU1-10, c	288	156	264	0.54	0.16	0.6470	0.91	27.646	0.78	3520	5	-9
CU1-11 r(3)	468	125	306	0.27	0.89	0.4919	0.89	19.184	0.80	3379	6	-27
CU1-12, r	51	27	35	0.53	4.48	0.5142	0.71	17.269	1.00	3143	11	-15
CU1-14, c	226	203	182	0.90	0.13	0.5363	0.96	24.238	0.91	3607	4	-27
CU1-15, c	93	65	65	0.70	0.90	0.4653	0.86	19.457	0.83	3487	7	-33
CU1-17, c	77	53	79	0.69	0.03	0.6863	0.87	30.429	1.0	3577	6	-6
CU1-19, c	948	656	287	0.69	2.09	0.2196	1.00	6.359	0.98	2905	8	-59
CU1-20, r	20	6	16	0.29	0.33	0.6216	0.73	22.881	3.24	3288	10	-4
CU1-21, c	118	117	123	0.99	1.08	0.6469	0.23	31.621	0.77	3726	47	-6
CU1-22, c	303	123	287	0.40	0.04	0.6734	0.96	29.992	0.78	3584	3	-8
CU1-26, r	92	52	83	0.56	0.04	0.6363	0.90	23.941	0.82	3323	5	-4
CU1-27, c	249	162	266	0.65	0.01	0.7151	0.89	31.894	0.79	3586	6	-2
CU1-28, c	110	87	119	0.80	0.02	0.7078	0.91	31.167	1.23	3567	5	-2
CU1-31, r	970	384	488	0.40	0.19	0.3688	0.87	14.149	0.79	3353	10	-43
CU1-32, c	99	92	100	0.94	0.74	0.6404	0.90	28.539	0.81	3585	5	-12
CU1-34, c	335	125	319	0.37	0.03	0.6813	0.98	29.856	1.06	3559	2	-6
CU1-35, r	31	10	25	0.31	1.88	0.5968	0.68	20.565	1.01	3184	12	-3
CU1-37, c	1818	145	379	0.08	0.45	0.1743	1.01	3.926	0.85	2490	20	-58
CU1-38, r	52	27	44	0.51	0.07	0.5926	0.83	22.023	0.73	3303	7	-9
CU1-39, c	320	217	385	0.68	0.01	0.7801	0.98	39.609	3.95	3784	2	-1
CU1-40, c	218	131	133	0.60	1.81	0.4258	0.70	15.797	0.94	3301	44	-26
CU1-41, r	23	17	21	0.75	0.09	0.6261	0.78	23.037	0.98	3288	9	-3

TABLE 4
(continued)

Spot number	Concentration, ppm			Th/U	f_{206} %(1)	Isotopic ratios				Age, Ma		Discordance
	U	Th	Pb			$^{206}Pb/^{238}U$	±σ	$^{207}Pb/^{235}U$	±σ	$^{207}Pb/^{206}Pb$	±σ	%
7-11, mica schist												
711-3, c	130	68	119	0.39	0.47	0.6354	0.71	28.716	0.85	3607	7	-13
711-6, c	226	93	219	0.36	0.22	0.6793	0.76	30.716	0.82	3607	4	-8
711-11, c	110	31	104	0.25	0.04	0.6813	0.71	29.242	0.82	3527	6	-5
711-13, c	239	8	217	0.03	0.02	0.6933	0.74	28.679	0.80	3470	4	-1
711-15, c	130	68	119	0.02	0.46	0.6319	0.82	27.138	0.93	3528	7	-11
711-16, c	520	184	304	0.21	0.74	0.4194	0.73	17.514	0.83	3485	6	-40
711-17, c	172	206	129	0.78	3.28	0.3016	9.35	9.166	9.74	2984	44	-35
711-20, c	95	46	95	0.74	0.47	0.4713	1.37	19.711	1.40	3487	4	-32
711-22, c	382	93	194	0.47	0.02	0.6893	0.73	29.617	0.78	3529	4	-4
711-25, c	282	308	163	0.16	0.52	0.3804	1.28	13.749	1.51	3259	13	-39
711-27, c	172	206	129	0.29	1.18	0.4019	3.19	16.610	3.24	3469	9	-40
5-88, mica schist												
588-4, c	593	288	370	0.26	1.11	0.4404	2.03	18.520	2.12	3496	9	-36
588-6, c	95	43	94	0.42	0.40	0.6918	0.71	30.520	0.77	3570	5	-5
588-7, c	437	182	434	0.40	0.02	0.6954	0.71	30.620	0.72	3567	2	-5
588-8, ic(4)	150	95	155	0.56	0.25	0.6816	0.71	33.309	0.76	3726	4	-11
588-8a, oc(5)	96	30	71	0.25	1.30	0.5200	0.75	22.604	0.87	3547	7	-27
588-8b, oc	330	89	272	0.22	0.28	0.5991	0.81	25.454	0.85	3512	4	-16
588-14, c	132	91	155	0.66	0.02	0.7621	0.76	38.709	0.81	3785	4	-3
588-15, r	491	135	272	0.16	0.67	0.4174	1.04	15.034	1.07	3254	4	-35
588-16, c	443	172	368	0.27	0.51	0.5955	0.71	25.549	0.76	3526	4	-17

Table 4

(continued)

Spot number	Concentration, ppm			Th/U	f_{206} %(1)	Isotopic ratios				Age, Ma		Discordance
	U	Th	Pb			$^{206}Pb/^{238}U$	±σ	$^{207}Pb/^{235}U$	±σ	$^{207}Pb/^{206}Pb$	±σ	%
92-218, paragneiss												
218-3, c	58	42	54	0.68	0.09	0.6274	0.72	24.702	0.80	3394	8	-10
218-4	82	56	67	0.63	1.10	0.5745	0.81	18.575	2.87	3083	28	-6
218-6	111	103	86	0.84	0.54	0.5198	0.77	16.663	0.84	3069	8	-15
218-9	153	79	128	0.49	0.09	0.6002	0.75	20.829	0.80	3195	8	-7
218-11	85	39	67	0.44	0.03	0.5851	0.71	18.579	0.84	3054	8	-4
218-17	821	156	227	0.06	4.48	0.2078	0.71	7.988	1.70	3356	15	-70
218-18	293	65	261	0.20	0.01	0.6578	0.84	26.940	0.89	3455	9	-7
218-19	223	68	207	0.29	0.02	0.6713	0.72	27.734	0.76	3468	7	-6
218-23	51	39	43	0.72	0.04	0.5865	0.72	18.962	0.85	3083	8	-4

1—f_{206}%, percentage of ^{206}Pb attributed to common Pb, which is calculated from measured ^{204}Pb; 2—c=optically distinct core; 3—r=optically distinct rim; 4—ic=inner core; 5—oc=outer core; 588a and b are repeated analyses.

one exception) have been identified in metasediments of the Belozerka and Verkhovtsevo greenstone belts. 3.3 Ga is also the oldest age determined for granite-gneisses of the Auli series, which is regarded as the basement to the greenstone belts (Samsonov and others, 1996). The dominant age component in the Belozersk series metasediments, 3.0 to 3.15 Ga (fig. 5B), is similar to the ages for volcanogenic parts and syntectonic granitoids in the greenstone belts. This is in agreement with the chemical compositions of sediments shown in the spider diagram in figure 3C. These data suggest that the contribution from volcano-plutonic sources to the sedimentary sequence was important. Volcanic rocks and granitoids of the belts, as well as the basement rocks, were eroded to provide material to the sediments.

The low uranium concentrations in most zircon grains indicate their origin from magmatic rocks of intermediate composition since zircons from acid volcanics (rhyolites) from the Belozerka series are extremely enriched in uranium, up to 3000 ppm (Samsonov and others, 1996).

In this study we present for the first time evidence of ages higher than 3.3 Ga in the Azov domain. The oldest ages have been identified in cores of detrital zircons from metasediments in the Soroki greenstone belt (figs. 7C and 7D).

Four zircon cores have $^{207}Pb/^{206}Pb$ ages in the range 3700 to 3800 Ma. Two of these, CU-1 spot 39 and 5-88 spot 14, are nearly concordant at 3785 Ma (table 4, fig. 6G, fig. 7A). CU-1 spot 8 is also nearly concordant, with a $^{207}Pb/^{206}Pb$ age of 3685 Ma (table 3, fig. 7A). Most cores are significantly discordant (fig. 7D), and about half of them have $^{207}Pb/^{206}Pb$ ages in the interval 3.65 to 3.4 Ga. It can be assumed that part of the radiogenic lead loss that caused this discordancy was mobilized during younger Archean and possibly Paleoproterozoic metamorphism, since such metamorphic overprint has been previously documented from the Azov Domain (Bibikova and others, 2008). This is also supported by the ages of zircon overgrowths presented in this study. Since such ancient lead loss results in a significant younging of measured $^{207}Pb/^{206}Pb$ ages, we regard the best age estimate for discordant cores with $^{207}Pb/^{206}Pb$ ages in the interval 3.3 to 3.5 Ga to be older than 3.5 Ga.

In summary, this study shows that Azov domain metasediments include an important, previously unidentified Paleoarchean component and also >3.6 Ga old material, demonstrating the existence of crust of such age in the provenance region for these rocks. If analogues are sought for early crustal development in other cratons, the Ukrainian Shield much resembles in its development the Pilbara craton in West Australia (Van Kranendonk and others, 2007).

The c. 3.2 to 3.3 Ga zircon overgrowths from the Soroki greenstone belt have probably formed during one or more metamorphic, zircon–forming event(s) in this age range. Based on the dominance of c. 3.3 Ga $^{207}Pb/^{206}Pb$ ages among the least discordant overgrowths, we take this as our best age estimate for the time of the earliest metamorphic event.

The wide range of Th/U ratios in zircons (fig. 8), points to different sources of the detritus and suggests that the age patterns presented here reflect the age components in the crust at the time of sedimentation and thus we presume that the ancient TTG complexes were much more expansive.

The Sm-Nd T_{DM} model ages of 3.1 to 3.3 Ga for Middle Dnepr domain metasediments (table 3) are consistent with the zircon age results, supporting the absence of significant pre-3.3 Ga age crust in this domain. For the Azov domain, the 3.3 to 3.4 Ga Sm-Nd T_{DM} model ages (table 3) demonstrate that the Soroki metasediments, and by inference the crust in this domain, in addition to the oldest components which in the

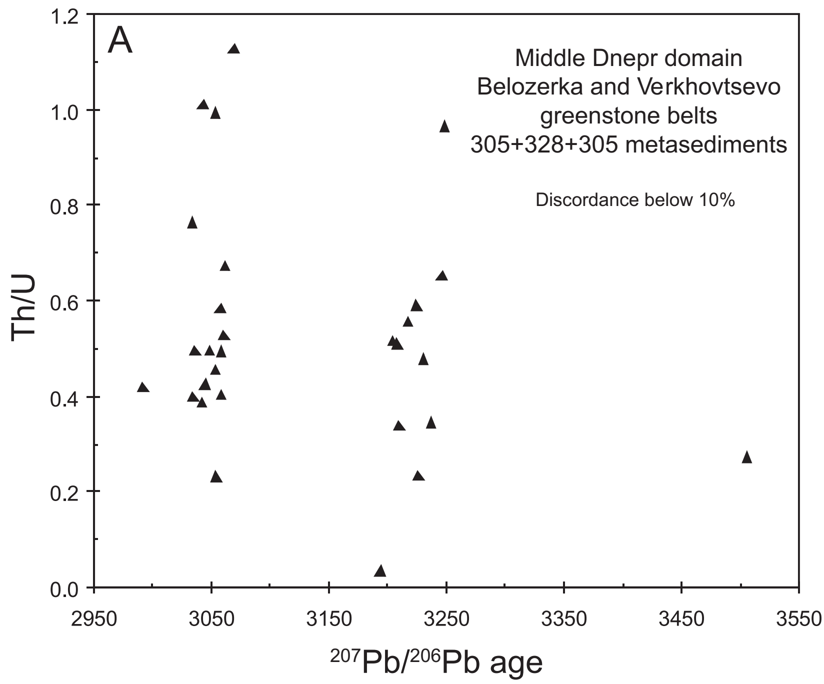

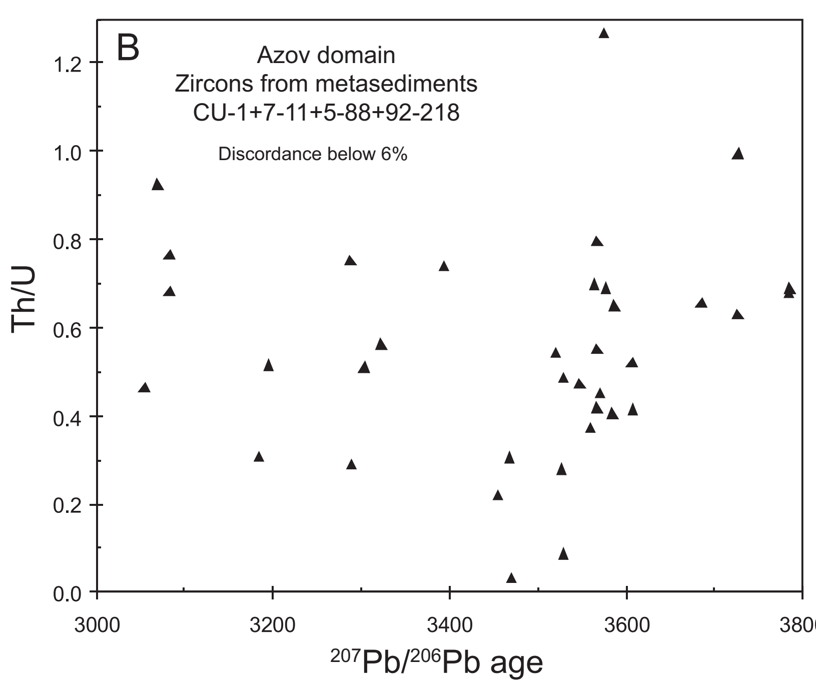

Fig. 8. Th/U versus $^{207}Pb/^{206}Pb$ age for zircons from metasediments: (A) Middle Dnepr domain. (B) Azov domain.

present study have been shown to be pre-3.5 Ga, also includes a large component of younger Paleo- to Mesoarchean material.

Thus, our study of metasedimentary rocks of the Ukranian Shield gives us an insight into the age and composition of Paleoarchean crust that now has largely disappeared from the Earth's surface.

This is a contribution to honor Alfred Kröner, whose work has always stimulated research of the early Earth.

ACKNOWLEDGMENTS

We thank Dr. Martin Whitehouse (Swedish Museum of Natural History) for help with SIMS and for valuable discussions of the results obtained at NORDSIM, Kerstin Lindén (Swedish Museum of Natural History) for kind help with SIMS analysis, and Ya. V. Bychkova (GEOKHI RAS) for ICP MS analysis. The research was partly supported by RFBR, Nos. 09-05-00226 and 08-05-90416 Russian-Ukrainian and Program 4 and 15 RAS. We kindly thank the reviewers of our manuscript Professor A. Trendall, Professor R. Pidgeon and the guest editor for constructive comments and recommendations, which permitted us to improve the manuscript.

The Nordsim laboratory is financed and operated by the Nordic countries under an agreement regulated by NOS-N. This is NORDSIM publication number 260.

Appendix

Table A1

Results of preliminary lead isotope study in zircons from metasediments, Middle Dnepr and Azov domains, Ukrainian Shield

Spot no	f_{206},%[(1)]	$^{207}Pb/^{206}Pb$ isotope ratios, corr.	± σ	$^{207}Pb/^{206}Pb$ ages, Ma	± σ
88-330, metasandstone, Belozerka greenstone belt, Belozerka series					
330-1	15.00	0.2403	3.64	3122	57
330-2	0.15	0.2521	0.63	3198	10
330-3	0.07	0.2316	0.93	3063	15
330-4	0.07	0.2301	0.55	3053	9
330-5	2.88	0.2535	0.89	3207	14
330-5a[(2)]	0.10	0.2324	0.81	3068	13
330-7	0.25	0.2270	1.11	3031	18
330-8	0.10	0.2297	0.42	3050	7
330-9	0.83	0.2299	0.67	3051	11
330-10	1.99	0.2701	0.46	3306	7
330-11	0.15	0.2328	0.68	3071	11
330-12	0.18	0.2313	0.75	3061	12
330-13	0.05	0.2311	0.41	3060	7
330-14	0.08	0.2303	0.52	3054	8
330-15	0.32	0.2267	0.72	3029	12
330-16	0.11	0.2610	0.63	3253	10
330-17	0.27	0.2288	0.72	3043	11
330-18	0.14	0.2278	0.87	3037	14
330-19	6.62	0.2280	1.73	3038	27
330-20	0.06	0.2309	0.68	3058	11
330-21	0.11	0.2605	0.79	3250	12
330-22	0.29	0.2285	0.47	3041	8
84-328, metasandstone, Belozerka greenstone belt, Belozerka series					
328-3	0.12	0.2315	0.80	3062	13
328-4	0.20	0.2497	0.53	3183	8
328-5	0.10	0.2575	0.79	3231	12
328-6	0.09	0.2291	0.75	3046	12
328-7	0.15	0.2290	0.68	3045	11
328-8	0.15	0.2596	0.77	3244	12
328-9	0.22	0.2399	0.94	3119	15
328-10	0.23	0.2285	0.52	3041	8
328-11	0.29	0.2299	0.66	3051	11
328-12	0.11	0.2298	0.90	3050	14
328-13	0.08	0.2323	0.44	3068	7
328-14	0.17	0.2321	0.75	3067	12
328-15	0.18	0.2305	0.57	3055	9
328-16	0.08	0.2317	0.80	3064	13
328-17	0.17	0.2286	0.70	3042	11
328-18	0.28	0.2583	0.92	3236	15
328-19	0.13	0.2292	0.78	3046	12
328-20	0.07	0.2303	0.44	3054	7
328-21	0.15	0.2272	0.57	3032	9
328-22	0.09	0.2521	0.50	3198	8
328-23	0.27	0.2274	0.60	3034	10
328-24	1.57	0.2251	1.19	3018	19
328-25	0.05	0.2306	0.41	3062	13
328-26	0.25	0.2275	0.50	3183	8
328-27	0.20	0.2275	0.98	3231	12
328-28	0.17	0.2284	0.87	3046	12
328-29	0.10	0.2305	0.54	3055	8
328-30	0.13	0.2310	0.53	3059	8

Table A1

(continued)

Spot no	f_{206},%[(1)]	$^{207}Pb/^{206}Pb$ isotope ratios, corr.	± σ	$^{207}Pb/^{206}Pb$ ages, Ma	± σ
88-305, metasandstone, Verkho vtsevo greenstone belt, Belozerka series					
305-1	1.28	0.2215	1.05	2991	17
305-2	0.12	0.2373	1.36	3102	22
305-3	0.86	0.2525	0.65	3200	10
305-4	0.06	0.2309	0.71	3059	11
305-5	0.35	0.2300	0.67	3052	11
305-6	0.78	0.2250	1.06	3017	17
305-7	0.05	0.3101	0.64	3522	10
305-8	0.04	0.2102	0.21	2907	4
305-9	0.02	0.2221	0.53	2996	9
305-10	0.03	0.2107	0.42	2911	7
305-11	0.05	0.2573	0.43	3230	7
305-12	0.12	0.2317	0.94	3064	15
305-13	0.07	0.2287	0.66	3043	11
305-14	0.03	0.2539	0.39	3209	6
305-15	0.05	0.2514	0.26	3194	4
CU-1, mica schist, Soroki greenstone belt					
CU1-1	0.06	0.3082	0.50	3512	8
CU1-2	0.45	0.3067	0.47	3504	7
CU1-3	0.20	0.3155	0.35	3548	5
CU1-4	2.41	0.2492	0.54	3180	9
CU1-5	0.06	0.3155	1.08	3548	17
CU1-6	0.06	0.3200	0.50	3570	8
CU1-7	0.75	0.3339	0.88	3635	13
CU1-8	0.06	0.3474	0.90	3696	14
CU1-9	0.08	0.3361	0.95	3645	15
CU1-10	0.21	0.3103	0.44	3522	7
CU1-11r[(3)]	0.46	0.2843	0.44	3387	7
CU1-12r	6.07	0.2449	1.28	3152	20
CU1-13	0.25	0.2302	1.04	3053	17
CU1-14	0.05	0.3349	0.39	3640	6
CU1-15	0.94	0.2965	0.88	3452	14
CU1-16	1.30	0.3049	0.48	3496	7
CU1-17	0.07	0.3181	0.65	3561	10
CU1-18	0.05	0.3174	0.55	3557	9
CU1-19	0.93	0.2294	5.94	3048	92
CU1-20r	0.62	0.2636	1.47	3268	23
CU1-21	1.23	0.3531	1.27	3721	19
CU1-22	0.06	0.3253	0.35	3595	5
CU1-23	0.04	0.3088	0.72	3515	11
CU1-24	0.10	0.2454	0.49	3156	8
CU1-25	0.06	0.2695	0.49	3303	8
CU1-26r	0.04	0.2690	0.68	3301	11
CU1-27	0.02	0.3201	0.33	3570	5
CU1-28	0.09	0.3141	1.04	3541	16
CU1-29	0.89	0.2773	0.58	3348	9
CU1-30	1.47	0.3103	0.94	3523	15
CU1-31r	0.17	0.3019	0.37	3480	6
CU1-32	0.92	0.3230	0.53	3584	8
CU1-33	0.05	0.2980	0.55	3460	9
CU1-34	0.07	0.3154	0.32	3547	5
CU1-35r	0.59	0.2834	1.63	3382	25

Table A1

(continued)

Spot no	f_{206},%[(1)]	$^{207}Pb/^{206}Pb$ isotope ratios, corr.	± σ	$^{207}Pb/^{206}Pb$ ages, Ma	± σ
		CU-1, mica schist, Soroki greenstone belt			
CU1-36	1.10	0.2344	0.84	3082	13
CU1-37	0.58	0.1694	3.67	2552	60
CU1-38r	0.13	0.2526	0.80	3201	13
CU1-39	0.02	0.3666	0.25	3778	4
CU1-40	0.39	0.3172	0.82	3556	13
CU1-41r	0.21	0.2640	1.76	3271	27
		7-11, mica schist, Soroki greenstone belt			
711-1	0.10	0.2736	0.45	3327	7
711-2	1.20	0.3037	1.38	3489	21
711-3	3.27	0.3397	1.09	3662	17
711-4	0.22	0.2558	0.82	3221	13
711-5	0.07	0.2460	0.44	3159	7
711-6	0.19	0.3271	0.30	3604	5
711-7	2.27	0.2899	0.52	3417	8
711-8	0.15	0.2575	0.64	3231	10
711-9	1.26	0.2796	0.52	3361	8
711-10	5.26	0.2018	0.61	2841	10
711-11	0.11	0.3045	0.81	3493	13
711-12	0.49	0.2748	0.49	3333	8
711-13	0.04	0.2984	0.38	3462	6
711-14	0.09	0.2371	0.56	3101	9
711-15	0.55	0.3051	0.34	3497	5
711-16	0.55	0.3091	0.29	3516	5
711-17	0.05	0.2350	0.38	3087	6
711-18	1.02	0.2225	0.69	2999	11
711-19	2.39	0.2695	0.44	3303	7
711-20	0.62	0.3055	0.43	3498	7
711-22	0.07	0.3068	0.56	3505	9
711-23	1.00	0.2126	0.31	2926	5
711-24	0.05	0.2362	0.52	3095	8
711-25	0.33	0.2686	0.52	3298	8
711-26	3.13	0.2550	0.56	3216	9
711-27	0.58	0.3120	0.43	3531	7
711-28	0.06	0.3093	0.52	3517	8
711-29	0.87	0.2452	0.34	3154	5
		5-88, mica schist, Soroki greenstone belt			
588-1	0.93	0.1888	0.53	2732	9
588-2	0.36	0.2954	0.46	3447	7
588-3	0.10	0.2605	0.65	3250	10
588-4	0.44	0.3282	0.27	3609	4
588-5	1.17	0.1601	3.39	2456	56
588-6	1.23	0.3143	0.56	3542	9
588-7	0.05	0.3187	0.36	3564	6
588-8	0.23	0.3523	0.48	3717	7
588-9	0.15	0.2506	0.87	3188	14
588-10	0.10	0.3581	0.48	3742	7
588-11	0.75	0.2804	0.83	3365	13
588-12	1.72	0.1747	1.33	2603	22
588-13	0.65	0.2202	0.56	2982	9
588-14	0.07	0.3653	0.63	3772	10
588-15r	0.93	0.2503	2.24	3186	35

Table A1

(continued)

Spot no	f_{206},%[(1)]	$^{207}Pb/^{206}Pb$ isotope ratios, corr.	± σ	$^{207}Pb/^{206}Pb$ ages, Ma	± σ
		5-88, mica schist, Soroki greenstone belt			
588-16	0.08	0.3196	0.48	3568	7
588-17	0.13	0.3055	0.66	3499	10
588-18	0.13	0.2778	0.54	3351	8
		92-218, paragneiss, Soroki greenstone belt			
218-1	0.01	0.1181	0.79	1928	14
218-2	0.01	0.1174	0.56	1916	10
218-3	0.19	0.2819	1.03	3374	16
218-4	0.14	0.2336	0.64	3077	10
218-5	0.07	0.2321	0.90	3067	14
218-6	0.33	0.2357	0.55	3091	9
218-7	11.00	0.1942	1.98	2778	32
218-8	0.05	0.2337	0.44	3077	7
218-9	0.12	0.2488	0.54	3177	9
218-10	0.07	0.2330	0.77	3073	12
218-11	0.09	0.2326	0.61	3070	10
218-12	5.05	0.2230	1.41	3002	23
218-13	0.44	0.2724	1.00	3320	16
218-14	1.08	0.2304	0.72	3055	12
218-15	1.78	0.2266	0.73	3028	12
218-16	0.81	0.2137	0.59	2934	10
218-17	0.32	0.3154	0.87	3547	13
218-18	0.05	0.2982	0.78	3461	12
218-19	0.05	0.2994	0.64	3467	10
218-20	0.07	0.2197	0.35	2978	6
218-21	0.69	0.2272	0.64	3033	10
218-22	0.34	0.2288	0.60	3044	10
218-23	0.14	0.2340	0.86	3080	14

1—f_{206}%, percentage of ^{206}Pb attributed to common Pb, which is calculated from measured ^{204}Pb; 2—a=repeated analysis; 3—r=rim.

References

Artemenko, G. V., 1997, The lower border of sedimentary rocks in Soroki and Fedorov graben synclines (Azov): Mineralogical Journal, B. 19, N6, p. 77–81.

Artemenko, G. V., Zhukov, G. V., and Klots, V. A., 1986, The lower border of Osipenkovo suite: Transaction of the Academy of Science of the USSR, Series B. N3, p. 3–5 (in Ukrainian).

Artemenko, G. V., Tatarinova, E. A., Popov, N. I., Razdorojny, V. F., and Dovbush, T. I., 2001, The age succession of Soroki greenstone structure formation: Geological Journal (Ukraine), N. 3, p. 78–84.

Bibikova, E. V., 1989, U-Pb geochronology of the early stages in development of ancient Shields: Moscow, Nauka, 140 p. (in Russian).

Bibikova, E. V., and Baadsgaard, H., 1986, Sm-Nd isotopic dating of the ancient formations of the Ukrainian shield and Omolon massif: Geochemistry International, N. 5, p. 601–618.

Bibikova, E. V., and Williams, I. S., 1990, Ion microprobe U-Th-Pb isotopic studies of zircons from three Early Precambrian areas in the USSR: Precambrian Research, v. 48, p. 203–221, doi:10.1016/0301-9268(90)90009-F.

Bibikova, E. V., Lobach-Zhuchenko, S. B., Artemenko, G. V., Claesson, S., and Kovalenko, A. V., 2008, Late Archean magmatic complexes of the Azov terrain Of the Ukrainian Shield: Geological setting, isotopic age and sources: Petrology, v. 16, n. 3, p. 227–247, doi:10.1134/S0869591108030016.

Bobrov, O. B., Sivornov, A. O., and Gursky, D. S., 2000, Geology and gold in Soroki greenstone structure (West Azov region): Dnepropetrovsk, Art-Press, 148 p., (in Ukrainian).

Claesson, S., Bibikova, E., Bogdanova, S., and Skobelev, V., 2006, Archaean Terranes, Palaeoproterozoic Reworking and Accretion in the Ukrainian Shield, East-European Craton, *in* Gee, D. G., and Stephenson, R. A., editors, European Lithosphere Dynamics: The Geological Society, London, Memoirs, v. 32, p. 645–654, doi:10.1144/GSL.MEM.2006.32.01.38.
Goldstein, S. J., and Jacobsen, S. B., 1988, Nd and Sr isotopic systematics of river water suspended material: implication for crustal evolution: Earth and Planetary Science Letters, v. 87, p. 249–265, doi:10.1016/0012-821X(88)90013-1.
Konkov, G. G., Maidanovich, I. A., and Rusakov, N. F., 1980, Geology of the Soroki tectonic zone (West Azov district): Tectonics and Stratigraphy, v. 19, p. 48–59 (in Russian).
Maas, R., and McCulloch, M. T., 1991, The provenance of Archean clastic metasediments in the Narryer Gneiss Complex, Western Australia: Trace element geochemistry, Nd isotopes, and U-Pb ages for detrital zircons: Geochimica et Cosmochimica Acta, v. 55, n. 7, p. 1915–1932, doi:10.1016/0016-7037(91)90033-2.
Martin, H., Smithies, R. H., Rapp, R., Moyen, J.-F., and Champion, D., 2005, An overview of adakite, tonalite-trondhjemite-granodiorite (TTG), and sanukitoid: relationships and some implications for crustal evolution: Lithos, v. 79, p. 1–24, doi:10.1016/j.lithos.2004.04.048.
Nance, W. B., and Taylor, S. R., 1976, Rare earth element patterns and crustal evolution—I. Australian post-Archean sedimentary rocks: Geochimica et Cosmochimica Acta, v. 40, p. 1539–1551, doi:10.1016/0016-7037(76)90093-4.
Nutman, A. P., 2001, On the scarcity of >3900 Ma detrital zircons in ≥3500 Ma metasediments: Precambrian Research, v. 105, p. 93–114, doi:10.1016/S0301-9268(00)00106-6.
Peck, W. H., Valley, J. W., Wilde, S. A., and Graham, C. M., 2001, Oxygen isotope ratios and rare earth elements in 3.3 to 4.4 Ga zircons: Ion microprobe evidence for high $\delta^{18}O$ continental crust and oceans in the Early Archean: Geochimica et Cosmochimica Acta, v. 65. p. 4215–4229, doi:10.1016/S0016-7037(01)00711-6.
Samsonov, A. V., Zhuravlev, D. Z., and Bibikova, Ye. V., 1993, Geochronology and petrogenesis of the Archean silicic volcanoplutonic series of the Verkhovtsevo Greenstone Structure, Ukraine: International Geology Review, v. 35, p. 1166–1181, doi:10.1080/00206819309465582.
Samsonov, A.,V., Chernyshev, I. V., Nutman, A. P., and Compston, W., 1996, Evolution of the Archaean Aulian gneiss complex, Middle Dnieper gneiss-greenstone terrain, Ulrainian Shield: SHRIMP U-Pb zircon evidence: Precambian Research, v. 78, p. 65–78, doi:10.1016/0301-9268(95)00069-0.
Scherbak, N. P., editor, 1985, Stratigraphic crossections in the Precambrian of the Ukrainian Shield: Kiev, Naukova Dumka, 168 p. (in Russian).
Scherbak, N. P., and Bartnitsky, E. N., 1995, Isotopic data of geological processes and the stratigraphic scheme of Precambrian of Ukrainian Shield: Geochemistry and Ore formation, v. 1, p. 3–24 (in Russian).
Scherbak, N. P., and Ponomarenko, F. N., 2000, Time succession of volcanism and granitic magmatism of Ukrainian Shield: Mineralogical Magazine, v. 22, n. 2/3, p. 12–24 (in Russian).
Scherbak, N. P., Zagnitko, V. N., Artemenko, G. V., and Bartnitsky, E. N., 1995, Geochronology of the main geological events in the Azov blok of USh: Geochemistry and ore formation, v. 21, p. 112–129 (in Russian).
Scherbak, N. P., Artemenko, G. V., Lesnaya, I. M., and Ponomarenko, A. N., 2005, Geochronology of the early Precambrian of the Ukrainian Shield. The Archean: Kiev, Naukova Dumka, 243 p. (in Russian).
Scherbakov, I. B., Petrology of the Ukrainian Shield: L'vov, 2005. 364 p., (in Russian).
Shcherbak, N. P., Bartnitsky, E. N., Bibikova, E. V., and Boiko, V. L., 1984, Age and Evolution of the Early Precambrian Continental Crust of the Ukrainian Shield, *in* Kröner, A., Hanson, G. N., and Goodwin, A. M., editors, Archaean Geochemistry: The Origin and Evolution of the Archaean Continental Crust: Berlin-Heidelberg-New York-Tokyo Springer-Verlag, p. 251–261.
Taylor, S. R., and McLennan, S. M., 1985, The continental crust: its composition and evolution: Oxford, Blackwell, 312 p.
Valley, J. W., Cavosie, A. J., Fu, B., Peck, W. H., and, Wilde, S. A., 2006, Comment on "Heterogeneous Hadean Hafnium: Evidence of continental crust at 4.4. to 4.5 Ga"; Science, v. 312, p. 1139–1140, doi:10.1126/science.1125301.
Van Kranendonk, M. J., Smithies, R. H., Hickman, A. H., and Champion, D. C., 2007, Secular tectonic evolution of Archaean continental crust: interplay between horizontal and vertical processes in the formation of the Pilbara Craton, Australia: Terra Nova, v. 19 (1), p. 1–38, doi:10.1111/j.1365-3121.2006.00723.x.
Whitehouse, M. J., and Kamber B. S., 2005, Assigning dates to thin gneissic veins in high-grade metamorphic terrane: A cautionary tale from Akilia, southwest Greenland: Journal of Petrology, v. 46, p. 291–318, doi:10.1093/petrology/egh075.
Whitehouse, M. J., Claesson, S., Sunde, T., and Vestin, J., 1997, Ion microprobe U-Pb zircon geochronology and correlation of Archaean gneisses from the Lewisian Complex of Gruinard Bay, northwest Scotland: Geochimica et Cosmochimica Acta, v. 61, p. 4429–4438, doi:10.1016/S0016-7037(97)00251-2.
Whitehouse, M. J., Kamber, B. S., and Moorbath, S., 1999, Age significance of U-Th-Pb zircon data from early Archaean rocks of west Greenland—a reassessment based on combined ion-microprobe and imaging studies: Chemical Geology, v. 160, p. 201–224, doi:10.1016/S0009-2541(99)00066-2.
Wilde, S. A., Valley, J. W., Peck, W. H., and Grahams, C. M., 2001, Evidence from detrital zircons for the existence of continental crust and oceans on the Earth 4.4 Gyr ago: Nature, v. 409, p. 175–178, doi:10.1038/35051550.